DESIGN OF A LAMINAR-FLOW-CONTROL SUPERCRITICAL AIRFOIL FOR A SWEPT WING

Dennis O. Allison and John R. Dagenhart

NASA Langley Research Center

SUMMARY

An airfoil was analytically designed and analyzed for a combination of supercritical flow and laminar flow control (LFC) by boundary-layer suction. A shockless inverse method was used to design an airfoil and an analysis method was used in lower-surface redesign work. The laminar-flow pressure distributions were computed without a boundary layer under the assumption that the laminar boundary layer would be kept thin by suction. Inviscid calculations showed that this 13.5-percent-thick airfoil has shockless flows for conditions at and below the design normal Mach number of 0.73 and the design section lift coefficient of 0.60, and that the maximum local normal Mach number is 1.12 at the design point. The laminar-boundary-layer instabilities can be controlled with suction but the undercut leading edge of the airfoil provides a low-velocity constant-pressure-coefficient region which is conducive to laminar flow without suction. Since the boundary layer can become turbulent due to intermittent adverse environmental conditions or suction failure, the lift can drop significantly. The airfoil was designed to be capable of lift recovery with no suction by the deflection of a small trailing-edge flap. The airfoil is not necessarily one of optimal performance because of the conservative constraints that were imposed on the design problem. However, it should provide a tool for experimental investigation of some fundamental problems relating to combined supercritical flow and laminar flow control.

INTRODUCTION

Laminar-flow-control work in the past has been done with conventional airfoils. Since then, efficient turbulent supercritical-type airfoils have been developed and they give large performance benefits when applied to turbulent aircraft. The current task was to design a laminar-flow-control (LFC) airfoil which maintains the advantages of a supercritical type of airfoil. The airfoil was analytically designed according to the concepts of Dr. Werner Pfenninger and Percy Bobbitt of Langley Research Center. The objective was to combine the advantages of supercritical-type airfoils and laminar flow control by suction for application to swept wings.

Four airfoil-design goals were established to carry out this objective. The first goal involves a set of two-dimensional target values as follows: a thickness-to-chord ratio of 0.13 or greater; a design normal Mach number of about 0.75; and a design section lift coefficient of about 0.60. The performance of a supercritical type of airfoil can be judged by the combination of these three parameters. The target values correspond to a good

turbulent supercritical airfoil. The first goal is to achieve a laminar airfoil which does not sacrifice any of these values. The second goal is to have shockless supercritical flow at and below the design Mach number and lift condition and to have a maximum local normal Mach number of about 1.15 at the design condition. A turbulent supercritical airfoil would have nearly shockless supercritical flow for Mach numbers and lift coefficients at and below the design condition. For laminar flow control a shockless configuration is desirable to minimize the suction requirement, which would be higher if laminarization through a shock wave were required. A maximum local normal Mach number of about 1.15 is high enough to allow good airfoil performance but low enough to minimize the tendency to form off-design shock waves. The third goal is to maintain a laminar boundary layer using suction. The fourth goal is for the airfoil to be capable of lift recovery in the unlikely event of suction failure.

To achieve these goals the airfoil was designed and analyzed by a process that is described in four steps. First, a laminar airfoil was designed for shockless supercritical flow over the upper surface. Next, the lower surface was redesigned for certain laminar-flow-control characteristics and a greater thickness-to-chord ratio. The third step was to analyze the airfoil for off-design shock formation with laminar flow control. The last step was to analyze the airfoil for lift loss and recovery with no LFC suction. The last two steps were, of course, performed iteratively with the first two.

SYMBOLS

The word "normal" refers to a direction normal to the leading edge of an untapered swept wing. The quantities described as normal were either input to or computed by a two-dimensional method.

C_p	normal pressure coefficient
$C_{p,sonic}$	sonic value of C_p
C_Q	suction coefficient, $\frac{\text{velocity into wall x density at wall}}{\text{free-stream velocity x free-stream density}}$
c_l	normal section lift coefficient
c_m	normal pitching-moment about the quarter-chord point
$M_{\ell,max}$	maximum local normal Mach number
M_n	normal component of free-stream Mach number
R	normal Reynolds number based on chord
t/c	normal thickness-to-chord ratio
x/c	nondimensional distance along airfoil chord

y/c	nondimensional normal distance perpendicular to airfoil chord
α	normal angle of attack
δ	normal flap deflection angle
Λ	sweep angle of untapered wing

Subscripts:

l.s.sep.	lower surface boundary layer separation
u.s.sep.	upper surface boundary layer separation

AIRFOIL DESIGN

Many steps were required in the airfoil design process but only two are described in this paper. Airfoil shapes and inviscid pressure distributions are shown in figure 1 for the two steps that are described. The airfoil was designed with no boundary layer assuming that the laminar boundary layer would be kept thin by suction. All the pressure distributions in this paper have a dashed line across them at the sonic value of the pressure coefficient. Pressure coefficients above the dashed line (more negative than $C_{p,sonic}$) correspond to local supersonic flow.

Shockless Supercritical Design

The airfoil in figure 1(a) is the most desirable of several airfoils designed using an early version (ref. 1) of the Bauer-Garabedian-Korn shockless inverse design method. (Ref. 2 contains updates to that version.) That method required many abstract parameters as inputs and produced the airfoil coordinates plus the pressure distribution.

The desirable part of this initial design is the upper surface which has a shockless region of supersonic flow covering about two-thirds of the chord length with a maximum local Mach number $M_{\ell,max}$ of 1.15. The pressure coefficient passes smoothly through the sonic value; in other words, there is no shock wave. Also the small slope in the pressure distribution at the sonic value means that the airfoil will be slow to form shock waves for nearby off-design Mach numbers and lift coefficients. Successive computer runs were made to maximize the combination of the design Mach number, lift, and thickness. The design Mach number M_n of 0.73 and the design lift coefficient c_l of 0.60 were considered acceptable but a thickness-to-chord ratio t/c higher than 0.126 was desired. This airfoil was designated SSC-73-06-126, which denotes shockless supercritical with design conditions of $M_n = 0.73$ and $c_l = 0.60$ with $t/c = 0.126$.

Laminar-Flow-Control Redesign

The airfoil in figure 1(b) is the result of redesigning the lower surface while maintaining the shockless supercritical characteristic of the upper surface. The redesign work was done using the Bauer-Garabedian-Korn-Jameson analysis method (ref. 2) which requires the airfoil coordinates as input and produces the pressure distribution. (Ref. 3 contains updates to the analysis method.) The maximum local Mach number $M_{\ell,max}$ for the redesigned airfoil is 1.12. This airfoil is designated LFC-73-06-135, which denotes laminar flow control with design conditions of $M_n = 0.73$ and $c_l = 0.60$ with $t/c = 0.135$. Coordinates for airfoil LFC-73-06-135 are given in table I.

Lower surface redesign.- The airfoil in figure 1(b) has a different type of lower surface, which might be desirable for certain laminar-flow-control features, and a higher thickness-to-chord ratio. The leading edge of the airfoil is undercut so that it produces a low-velocity region of near-constant pressure coefficient which is conducive to laminar flow without suction. This might allow a leading-edge device to be installed in the lower surface since no suction would be required in this region and the low velocities might permit laminar flow over local surface discontinuities which could arise from the leading-edge device. Another benefit is that the small leading-edge radius alleviates the spanwise leading-edge contamination problem. Also, the magnitude of the pitching moment is slightly lower for the redesigned airfoil (reduced from $c_m = -0.12$ to $c_m = -0.10$). The center of the airfoil was thickened until a very small region of supersonic flow developed, while the front and rear were thinned so as to maintain the design section lift coefficient c_l of 0.60. As a result, the area inside the airfoil remained about the same. This unusual shape for the lower surface was designed with careful consideration of the laminar-boundary-layer instabilities.

Laminar-boundary-layer instabilities.- Three types of laminar-boundary-layer instabilities were considered as indicated in figure 2. The Tollmien-Schlichting instability predominates in the region of small adverse pressure gradient, which covers about one-half of the upper surface. The cross-flow instability is due to wing sweep and predominates in the four steep-pressure-gradient regions of the upper and lower surfaces. The Tollmien-Schlichting and cross-flow disturbance growths were computed by the method described in reference 4. The Taylor-Goertler instability is due to centrifugal effects in the concave regions of the lower surface, and the disturbance growth was computed by the method of Smith (ref. 5).

To maintain a laminar boundary layer the growth of boundary-layer disturbances must be kept within acceptable limits. The airfoil had to be redesigned to control the cross-flow and Taylor-Goertler instabilities. This was done by an iterative process of successively changing the airfoil shape and recomputing the disturbance growths. Another iterative process was required between an assumed suction distribution and the cross-flow instability growth for each airfoil shape. Also, each time the airfoil was reshaped the coordinates had to be adjusted to maintain fairness of the surface.

Contrary to what might be expected, the cross-flow disturbance growth depends more on the time spent in the steep gradient than on the steepness of the gradient. Therefore, it was controlled by confining each steep gradient to a short distance along the chord. That is why the four gradients indicated by the label "cross-flow" in figure 2 are so steep. Similarly, the Taylor-Goertler disturbance growth depends more on the time spent in a concave curvature region than on the magnitude of the curvature. Control was effected by confining each concave curvature to a short distance along the chord. As a result the two concave curvature regions of the lower surface have high curvatures and two dips (labeled Taylor-Goertler) appear in the pressure distribution in figure 2.

LFC suction distribution.- Current plans are to investigate a swept model of an airfoil similar to LFC-73-06-135 with suction in the Ames 12-foot pressure wind tunnel. Such an investigation will require a very complicated wind-tunnel wall liner (design procedure discussed by Newman and Anderson in ref. 6). Figure 3 shows a suction distribution suitable for maintaining laminar flow over airfoil LFC-73-06-135 under a set of proposed test conditions. The two-dimensional Mach number, lift coefficient, and Reynolds number are: $M_n = 0.73$, $c_l = 0.60$, and $R = 10 \times 10^6$. A sweep angle Λ of 35° was chosen to produce cross flows equivalent to those of a full-scale aircraft at cruise altitude with a lower sweep. The suction coefficient C_Q is plotted against non-dimensional distance along the chord. The suction shown is sufficient to keep the laminar-boundary-layer disturbance growths within acceptable bounds according to the criteria set forth in references 4 and 5. Since growth is a cumulative quantity, a different suction distribution could be used to limit the growths to the same bounds.

The suction distribution in figure 3 will be discussed in terms of the pressure distribution in figure 2. A low level of suction is shown over about one-half of the upper surface where the Tollmien-Schlichting instability predominates and the adverse pressure gradient is small. Higher suction levels are shown in the front and rear of the upper surface where the cross-flow instability predominates and the pressure gradients are steep. Only a narrow spike is used in the front since the steep gradient is confined to a short distance along the chord. In the rear the suction coefficient builds up to a higher level since the steep pressure gradient is spread over a larger distance along the chord. On the lower surface, it is desirable to have no suction in the leading-edge region to improve the feasibility of a leading-edge device; no suction is required there since the steep pressure gradient is confined to a very short distance along the chord and the following gradient is nearly zero. Significant levels of suction are shown over most of the lower surface where there are two steep pressure gradients and the cross-flow instability predominates. The level could be lowered in the center of the lower surface but it would be coupled with increased levels elsewhere. No suction is shown in the trailing-edge region of the lower surface since the pressure gradient suddenly reverses itself at $x/c = 0.81$ and sets up a counter cross flow which works against the previous cross flow. No additional suction is required for the Taylor-Goertler instability since it is controlled by airfoil shaping as explained earlier rather than by suction.

AIRFOIL ANALYSIS

Airfoil analysis was performed to study shock-wave formation at off-design conditions with laminar flow control and to study lift loss and recovery with suction failure. A large number of calculations were made using the analysis method of reference 2, and a few samples were selected for discussion in the following paragraphs.

Off-Design Shock Formation With LFC

Effects of off-design Mach numbers, off-design lift coefficients and deflections of a small trailing-edge flap are illustrated by the inviscid pressure distributions for airfoil LFC-73-06-135 which are shown in figures 4 to 6. Shock-wave formation at off-design conditions was studied using laminar-flow pressure distributions which were computed with no boundary layer assuming that the laminar boundary layer would be kept thin by suction.

Off-design Mach numbers.- Figure 4 shows laminar-flow pressure distributions for off-design Mach numbers at the design lift coefficient c_l of 0.60. The design pressure distribution is shown at the lower left for reference. The only shock wave which appears in this figure is for $M_n = 0.75$, which is above the design value of $M_n = 0.73$. For a poorly designed upper surface, a double shock wave could form near the rear of the supersonic zone for a Mach number just below the design value, and it would move forward for lower Mach numbers. No such shock waves appear for the lower Mach number of 0.70. The airfoil does not have off-design shock-wave formation for Mach numbers below the design point.

Off-design lift coefficients.- Figure 5 shows laminar-flow pressure distributions for off-design lift coefficients at the design Mach number M_n of 0.73. The design pressure distribution is again shown at the lower left for reference. The only shock wave which appears in this figure is for $c_l = 0.70$, which is above the design value of $c_l = 0.60$. It should be noted that for a poorly designed upper surface, a double shock wave often forms near the rear of the supersonic zone for a lift coefficient just below the design value, and moves forward as the lift coefficient is decreased. No shock wave appears for the lower lift coefficient of 0.50. The airfoil does not have off-design shock-wave formation for lift coefficients below the design point until the lift coefficient reaches about 0.30. For lift coefficients of 0.30 and lower a shock wave forms on the lower surface for a Mach number of 0.73.

Small trailing-edge flap.- The lift coefficient was controlled in figure 5 by angle-of-attack variations from -0.8° to 0.5°, but it can be controlled by deflections of a small trailing-edge flap. Figure 6 shows laminar flow pressure distributions with the angle of attack held at its design value of $\alpha = 0.1^\circ$ for -3.4° to 1.6° deflections of a 5-percent-chord trailing-edge flap to produce the four lift coefficients shown in figure 5. The pressure distributions in figure 6 show no shock-wave formation until the lift

coefficient is raised above the design value. For the lift coefficient c_l of 0.70 an indication of only a weak shock wave appears. This shows that the lift coefficient can be controlled by deflecting a small trailing-edge flap without spoiling the shockless nature of the topside pressures at lift coefficients below design.

Lift Behavior With Suction Failure

The loss and recovery of lift in the unlikely event of suction failure is illustrated for airfoil LFC-73-06-135 in figures 7 and 8. Suction failure was simulated by computing pressure distributions with a turbulent boundary layer for a wind-tunnel Reynolds number R of 10×10^6 starting at x/c = 0.02 on both the upper and lower surfaces of the airfoil. It is possible to have a turbulent boundary layer with suction but these calculations are for the worst case of a turbulent boundary layer with no LFC suction.

Lift loss.- The calculations in figure 7 are for lift loss at the design Mach number and with the angle of attack held at its design value of 0.1°. The inviscid design pressure distribution simulating LFC suction is shown in figure 7(a) for reference. The pressure distribution with a turbulent boundary layer simulating suction failure is shown in figure 7(b) where $c_l = 0.28$. For a flight Reynolds number R of 40×10^6 a slightly higher lift coefficient c_l of 0.32 is predicted.

The boundary-layer separation predictions (fig. 7(b)) are x/c = 0.95 for the upper surface and x/c = 0.75 for the lower surface. The analysis method is conservative in that it tends to predict separation earlier than it would actually occur. The separated region on the upper surface would probably cover less than 5 percent of chord. On the lower surface, separation would probably occur behind x/c = 0.75 but the analysis method cannot predict reattachment. However, the favorable pressure gradient which starts at about x/c = 0.82 is conducive to reattachment and the flow will probably reattach on the lower surface well before reaching the trailing edge. The prediction of $c_l = 0.28$ may not be accurate since the reattachment point is uncertain, but the lift coefficient is not very sensitive to lower surface changes. Therefore, it is believed that about one-half of the design lift coefficient may be lost due to suction failure.

Lift recovery.- Two ways were considered by which the lift might be recovered with no suction. The results in figure 8 were calculated with a turbulent boundary layer for the design Mach number and the same wind-tunnel Reynolds number as in figure 7. The lift coefficient is restored to 0.60 in figure 8(a) by angle of attack and in figure 8(b) by the deflection of a 5-percent-chord trailing-edge flap. When the lift is recovered by a 1.8° angle of attack (fig. 8(a)), a shock wave forms and the upper-surface separation point moves forward to x/c = 0.91, both of which cause additional drag. Also, the lift calculation may not be valid when the upper-surface separation point moves forward from x/c = 0.95. When the lift is recovered by an 8° deflection of a 5-percent-chord trailing-edge flap (fig. 8(b)) no shock wave

forms and the pressure distribution is similar to the design pressure distribution (fig. 7(a)). For the flap-deflection case (fig. 8(b)), the upper-surface separation remained confined to the last 5 percent of chord. On the lower surface, separation would probably occur behind $x/c = 0.76$ and would probably reattach before $x/c = 0.95$ where the flap is located. It is believed that the airfoil is capable of lift recovery but an experimental investigation is needed to determine what deflection angle is required to recover the lift coefficient of 0.60.

CONCLUDING REMARKS

Airfoil LFC-73-06-135 has been analytically designed and analyzed for combined supercritical flow and laminar flow control and achieves the four goals which were mentioned in the Introduction. This airfoil has a thickness-to-chord ratio of 0.135 which is a little higher than the target value, a design normal Mach number of 0.73 which is a little lower than the target value, and a design section lift coefficient of 0.60 which is equal to the target value. It has shockless supercritical flow for Mach number and lift conditions at and below the design values and the maximum local normal Mach number at the design condition is 1.12. It has laminar-boundary-layer instabilities which can be controlled by suction. In the unlikely event of suction failure, it is capable of lift recovery by the deflection of a small trailing-edge flap.

Because of the conservative constraints that were imposed on the design problem, airfoil LFC-73-06-135 does not have as high a design lift coefficient or Mach number as possible. This airfoil, however, with its maximum local Mach number being higher than for previously tested subsonic airfoils with laminar flow control and with its undercut leading edge, provides a tool for investigating some fundamental problems such as that of maintaining laminar flow through a region of significant supercritical flow. Current plans are for experimental validation of an airfoil similar to LFC-73-06-135 in the Ames 12-foot pressure wind tunnel using a swept model with a small trailing-edge flap.

REFERENCES

1. Bauer, F.; Garabedian, P.; and Korn, D.: A Theory of Supercritical Wing Sections, With Computer Programs and Examples. Volume 66 of Lecture Notes in Economics and Mathematical Systems, Springer-Verlag, 1972.

2. Bauer, Frances; Garabedian, Paul; Korn, David; and Jameson, Antony: Supercritical Wing Sections II. Volume 108 of Lecture Notes in Economics and Mathematical Systems, Springer-Verlag, 1975.

3. Bauer, Frances; Garabedian, Paul; and Korn, David: Supercritical Wing Sections III. Volume 150 of Lecture Notes in Economics and Mathematical Systems, Springer-Verlag, 1977.

4. Srokowski, Andrew J.; and Orszag, Steven A.: Mass Flow Requirements for LFC Wing Design. [Paper] 77-1222, American Inst. of Aeronaut. & Astronaut., Aug. 1977.

5. Smith, A. M. O.: On the Growth of Taylor-Görtler Vortices Along Highly Concave Walls. Quart. Appl. Math., vol. XIII, no. 3, Oct. 1955, pp. 233-262.

6. Newman, Perry A.; and Anderson, E. Clay: Analytical Design of a Contoured Wind-Tunnel Liner for Supercritical Testing. Advanced Technology Airfoil Research, Volume I, CP-2045, 1978.

TABLE I.- COORDINATES FOR AIRFOIL LFC-73-06-135

Upper surface		Lower surface	
x/c	y/c	x/c	y/c
0.00000	0.01200	0.00000	0.01200
.00071	.01593	.00091	.00923
.00183	.01873	.00274	.00758
.00348	.02156	.00556	.00606
.00576	.02441	.00930	.00456
.00865	.02725	.01388	.00309
.01217	.03006	.01933	.00167
.01633	.03282	.02562	.00030
.02112	.03553	.03276	-.00104
.02655	.03815	.04076	-.00237
.03263	.04068	.04959	-.00370
.03937	.04310	.05925	-.00507
.04678	.04541	.06971	-.00647
.05486	.04761	.08095	-.00793
.06361	.04970	.09265	-.00942
.07304	.05171	.10537	-.01105
.08312	.05364	.11880	-.01276
.09384	.05549	.13290	-.01456
.10518	.05727	.14763	-.01645
.11711	.05897	.16293	-.01840
.12962	.06059	.17874	-.02070
.14268	.06214	.19497	-.02360
.15628	.06362	.21151	-.02718
.17038	.06501	.22822	-.03119
.18497	.06632	.24495	-.03537
.20002	.06754	.26150	-.03954
.21552	.06867	.27823	-.04377
.23142	.06972	.29409	-.04748
.24772	.07067	.30978	-.05062
.26438	.07153	.32552	-.05318
.28138	.07230	.34148	-.05521
.29870	.07297	.35767	-.05682
.31629	.07353	.37410	-.05808
.33414	.07400	.39072	-.05903
.35223	.07437	.40753	-.05970
.37051	.07463	.42446	-.06009
.38897	.07479	.44150	-.06022
.40757	.07484	.45860	-.06008
.42628	.07478	.47574	-.05965
.44508	.07461	.49289	-.05892

Upper surface		Lower surface	
x/c	y/c	x/c	y/c
0.46394	0.07434	0.51005	-0.05787
.48283	.07395	.52720	-.05648
.50172	.07345	.54435	-.05474
.52058	.07283	.56150	-.05264
.53938	.07210	.57868	-.05017
.55809	.07125	.59590	-.04735
.57669	.07028	.61318	-.04419
.59515	.06919	.63053	-.04073
.61345	.06797	.64796	-.03698
.63155	.06664	.66500	-.03308
.64943	.06517	.68000	-.02946
.66708	.06358	.70000	-.02450
.68447	.06186	.72000	-.01954
.70158	.06001	.74000	-.01458
.71839	.05803	.76000	-.00962
.73487	.05593	.78000	-.00466
.75103	.05371	.79000	-.00218
.76683	.05136	.80000	.00020
.78227	.04889	.80750	.00165
.79733	.04631	.81500	.00255
.81201	.04361	.82250	.00297
.82630	.04080	.83000	.00307
.84000	.03791	.83500	.00303
.85000	.03570	.84000	.00299
.86000	.03349	.85000	.00290
.87000	.03128	.86000	.00281
.88000	.02907	.87000	.00272
.89000	.02686	.88000	.00263
.90000	.02465	.89000	.00254
.91000	.02244	.90000	.00245
.92000	.02023	.91000	.00236
.93000	.01802	.92000	.00227
.94000	.01581	.93000	.00218
.95000	.01360	.94000	.00209
.96000	.01139	.95000	.00200
.97000	.00918	.96000	.00191
.98000	.00697	.97000	.00182
.99000	.00476	.98000	.00173
1.00000	.00255	.99000	.00164
		1.00000	.00155

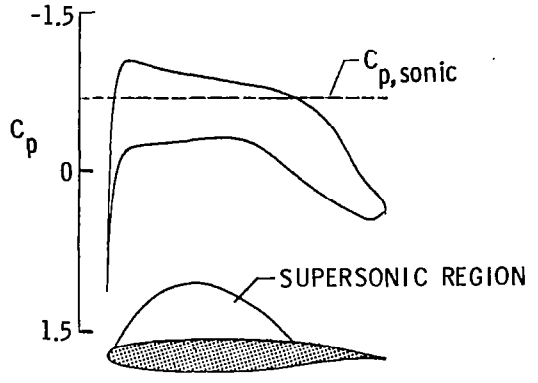

(a) Shockless supercritical design. Airfoil SSC-73-06-126; t/c = 0.126; $M_{\ell,max}$ = 1.15.

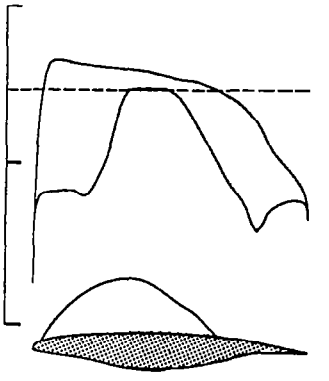

(b) Laminar-flow-control redesign. Airfoil LFC-73-06-135; t/c = 0.135; $M_{\ell,max}$ = 1.12.

Figure 1.- Airfoils and inviscid pressure distributions for two steps in design process with M_n = 0.73 and c_l = 0.60.

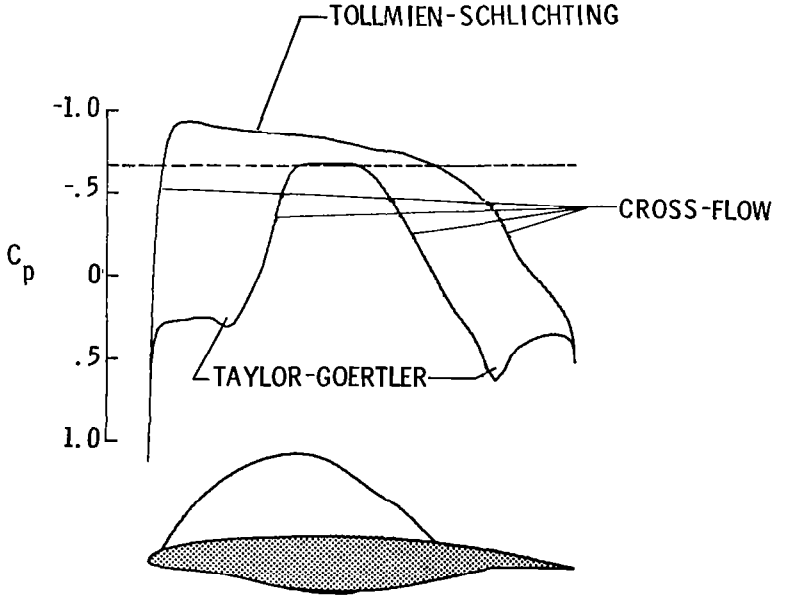

Figure 2.- Laminar-boundary-layer instabilities for airfoil LFC-73-06-135 with M_n = 0.73 and c_l = 0.60.

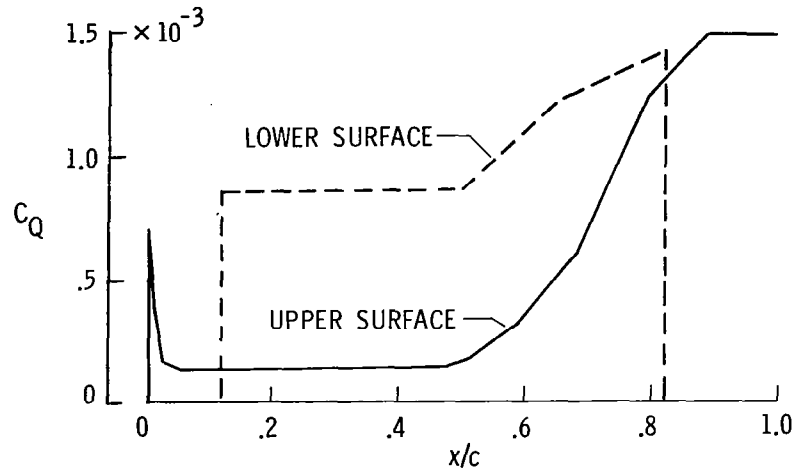

Figure 3.- Laminar-flow-control suction distribution for airfoil LFC-73-06-135 with M_n = 0.73, c_l = 0.60, R = 10 × 10^6, and Λ = 35°.

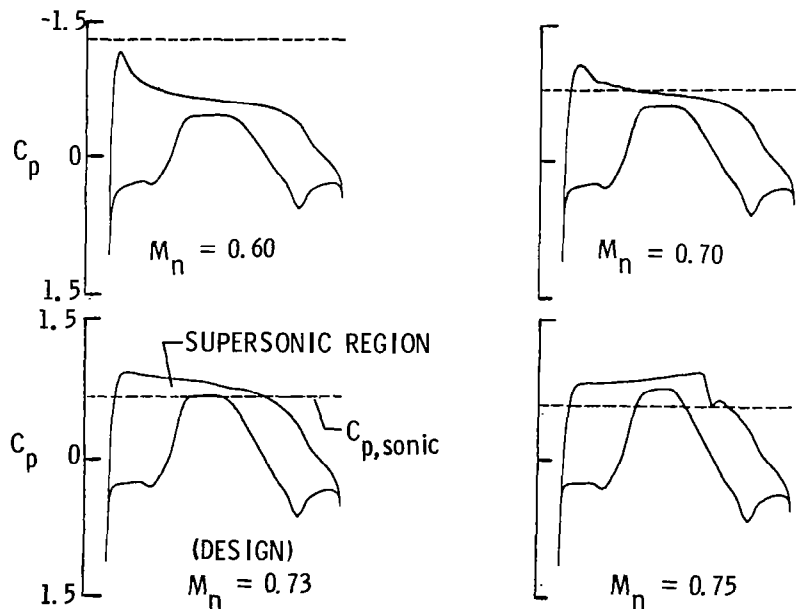

Figure 4.- Inviscid pressure distributions for off-design Mach numbers at design lift coefficient c_l of 0.60 for airfoil LFC-73-06-135.

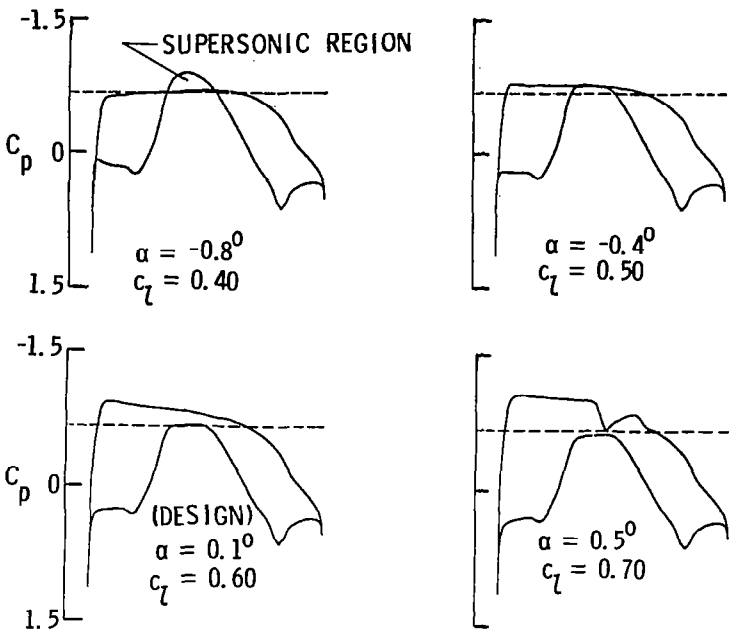

Figure 5.- Inviscid pressure distributions for off-design lift coefficients at design Mach number M_n of 0.73 for airfoil LFC-73-06-135.

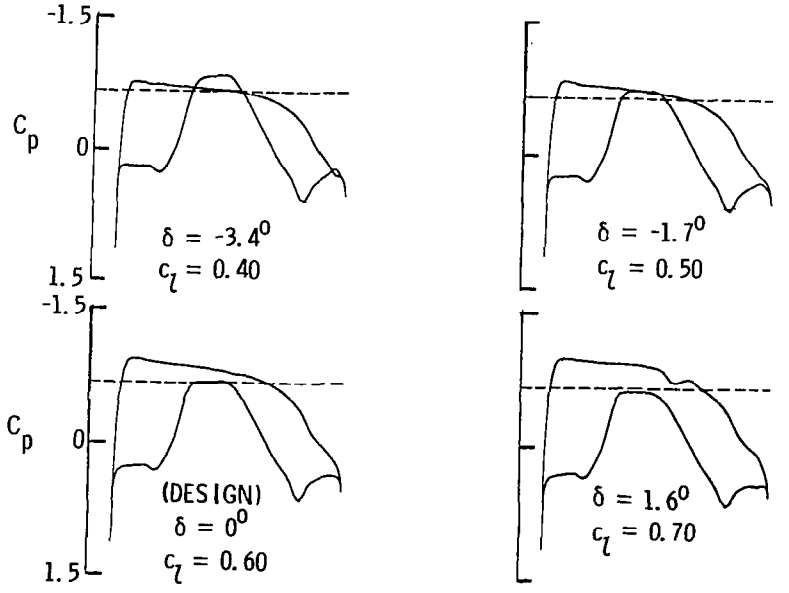

Figure 6.- Inviscid pressure distributions for deflections of a 5-percent-chord trailing-edge flap at design conditions of M_n = 0.73 and α = 0.1° for airfoil LFC-73-06-135.

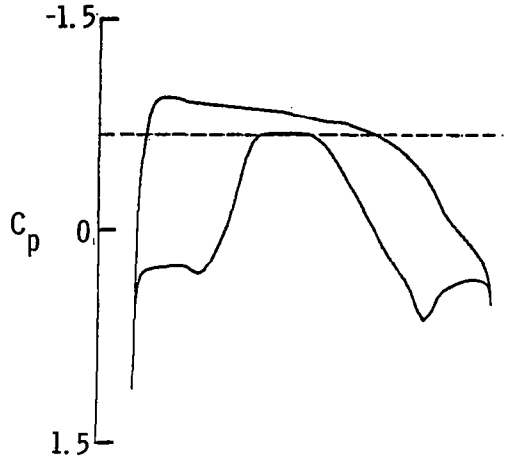

(a) Inviscid design pressure distribution simulating LFC suction for $c_l = 0.60$.

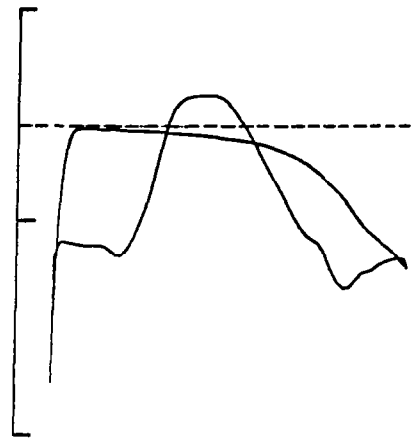

(b) Pressure distribution with turbulent boundary layer for $R = 10 \times 10^6$ simulating no LFC suction with $c_l = 0.28$, $(x/c)_{u.s.sep.} = 0.95$, and $(x/c)_{l.s.sep.} = 0.75$.

Figure 7.- Pressure distributions which show lift loss due to suction failure at design conditions of $M_n = 0.73$ and $\alpha = 0.1^o$.

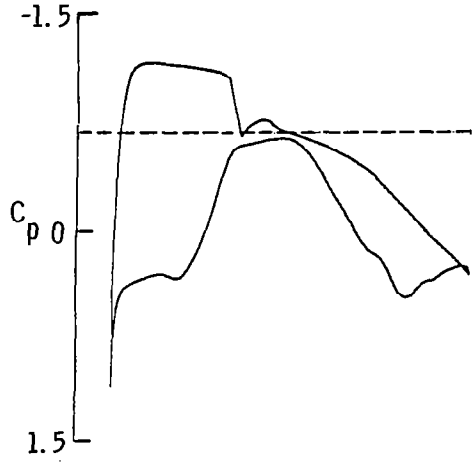

(a) Lift recovery by angle of attack for $\alpha = 1.8^o$ and $\delta = 0^o$ with $(x/c)_{u.s.sep.} = 0.91$ and $(x/c)_{l.s.sep.} = 0.75$.

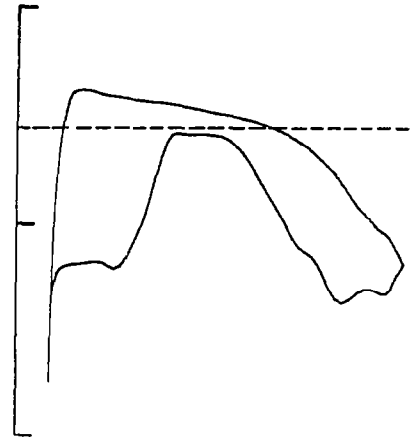

(b) Lift recovery by 5-percent-chord trailing-edge flap for $\alpha = 0.1^o$ and $\delta = 8.0^o$ with $(x/c)_{u.s.sep.} = 0.95$ and $(x/c)_{l.s.sep.} = 0.76$.

Figure 8.- Pressure distributions with turbulent boundary layer for $R = 10 \times 10^6$ which show lift recovery with suction failure at design conditions of $M_n = 0.73$ and $c_l = 0.60$.